# Structural Characterization of MAO and Related Aluminum Complexes. 1. Solid-State $^{27}$Al NMR with Comparison to EFG Tensors from ab Initio Molecular Orbital Calculations

**Pamela L. Bryant,[†] Chris R. Harwell,[†] Anthony A. Mrse,[†] Earl F. Emery,[†] Zhehong Gan,[‡] Tod Caldwell,[‡] Arneil P. Reyes,[‡] Philip Kuhns,[‡] David W. Hoyt,[§] Larry S. Simeral,*,[∥] Randall W. Hall,*,[†,⊥] and Leslie G. Butler*,[†]**

*Department of Chemistry, Louisiana State University, Baton Rouge, Louisiana 70803,*
*National High Magnetic Field Laboratory, Tallahassee, Florida 32310, Environmental Molecular Science*
*Laboratory, Pacific Northwest National Laboratory, Richland, Washington 99352,*
*Albemarle Corporation, P.O. Box 14799, Baton Rouge, Louisiana 70898,*
*and Department of Physics & Astronomy, Louisiana State University, Baton Rouge, Louisiana 70803*

*Received April 30, 2001. Revised Manuscript Received August 10, 2001*

**Abstract:** Experimental and ab initio molecular orbital techniques are developed for study of aluminum species with large quadrupole coupling constants to test structural models for methylaluminoxanes (MAO). The techniques are applied to nitrogen- and oxygen-containing complexes of aluminum and to solid MAO isolated from active commercial MAO preparations. (Aminato)- and (propanolato)aluminum clusters with 3-, 4-, and 6-coordinate aluminum sites are studied with three $^{27}$Al NMR techniques optimized for large $^{27}$Al quadrupole coupling constants: field-swept, frequency-stepped, and high-field MAS NMR. Four-membered (aminato)-aluminum complexes with $AlN_4$ coordination yield slightly smaller $C_q$ values than similar $AlN_2C_2$ sites: 12.2 vs 15.8 MHz. Planar 3-coordinate $AlN_2C$ sites have the largest $C_q$ values, 37 MHz. In all cases, molecular orbital calculations of the electric field gradient tensors yields $C_q$ and $\eta$ values that match with experiment, even for a large hexameric (aminato)aluminum cage. A $D_{3d}$ symmetry hexaaluminum oxane cluster, postulated as a model for MAO, yields a calculated $C_q$ of −23.7 MHz, $\eta = 0.7474$, and predicts a spectrum that is too broad to match the field-swept NMR of methylaluminoxane, which shows at least three sites, all with $C_q$ values greater than 15 MHz but less than 21 MHz. Thus, the proposed hexaaluminum cluster, with its strained four-membered rings, is not a major component of MAO. However, calculations for dimers of the cage complex, either edge-bridged or face-bridged, show a much closer match to experiment. Also, MAO preparations differ, with a gel form of MAO having significantly larger $^{27}$Al $C_q$ values than a nongel form, a conclusion reached on the basis of $^{27}$Al NMR line widths in field-swept NMR spectra acquired from 13 to 24 T.

## Introduction

The structure of methylaluminoxane (MAO) is unknown. It may be a dynamic mixture of linear, ring, and cage complexes, all formed from methylaluminum oxane subunits ($CH_3AlO$) during the controlled hydrolysis of trimethylaluminum.[1−7] A knowledge of the MAO structure is important for the continued development of new-generation polyolefin catalysts.[8−10] Ziegler−Natta catalysts are formed from zirconocenes and various amounts of MAO, ranging from Zr:Al ratios of 1:1 up to 1:100 or even larger.[5] For 20 years, a hypothesis for the catalytic activity has been based on a presumed special aluminum site in MAO.[11] For this reason, $^{27}$Al NMR spectroscopy has been often attempted.[12−15] Unfortunately, it is very difficult to acquire reliable $^{27}$Al NMR spectra of MAO. Previous studies determined the $^{27}$Al isotropic chemical shift of MAO to be 149−153 ppm with a fwhm of 1750 Hz which virtually coincides

---

* To whom correspondence should be addressed.

[†] Department of Chemistry, Louisiana State University.

[‡] National High Magnetic Field Laboratory.

[§] Environmental Molecular Science Laboratory, Pacific Northwest National Laboratory.

[∥] Albemarle Corporation.

[⊥] Department of Physics & Astronomy, Louisiana State University.

(1) Mason, M. R.; Smith, J. M.; Bott, S. G.; Barron, A. R. *J. Am. Chem. Soc.* **1993**, *115*, 4971−84.

(2) Sinn, H. J. *Macromol. Symp.* **1995**, *97*, 27−52.

(3) Beard, W. R.; Blevins, D. R.; Imhoff, D. W.; Kneale, B.; Simeral, L. S. In *International Polyethylene Conference, Polyethylene: New Technology, New Markets*; Institute of Materials: London, 1997.

(4) Imhoff, D. W.; Simeral, L. S.; Sangokoya, S. A.; Peel, J. H. *Organometallics* **1998**, *17*, 1941−5.

(5) Chen, E. Y.-X.; Marks, T. J. *Chem. Rev.* **2000**, *100*, 1391−434.

(6) Ystenes, M.; Eilertsen, J. L.; Liu, J.; Ott, M.; Rytter, E.; Støvneng, J. A. *J. Polym. Sci., Part A: Polym. Chem.* **2000**, *38*, 3106−27.

(7) Roesky, H. W.; Walawalkar, M. G.; Murugavel, R. *Acc. Chem. Res.* **2001**, *34*, 201−11.

(8) Brintzinger, H. H.; Fischer, D.; Mülhaupt, R.; Rieger, B.; Waymouth, R. M. *Angew. Chem., Int. Ed. Engl.* **1995**, *34*, 1143−70.

(9) Carlson, E. D.; Krejchi, M. T.; Shah, C. D.; Terakawa, T.; Waymouth, R. M.; Fuller, G. G. *Macromolecules* **1998**, *31*, 5343−51.

(10) Charpentier, P. A.; Zhu, S.; Hamielec, A. E.; Brook, M. A. *Polymer* **1998**, *39*, 6501−11.

(11) Sinn, H.; Kaminsky, W.; Vollmer, H. J.; Woldt, R. *Angew. Chem., Int. Ed. Engl.* **1980**, *19*, 390−2.

(12) Kriz, O.; Casensky, B.; Lycka, A.; Fusek, J.; Hermanek, S. *J. Magn. Reson.* **1984**, *60*, 375−81.

(13) Sugano, T.; Matsubara, K.; Fujita, T.; Takahashi, T. *J. Mol. Catal.* **1993**, *82*, 93−101.

(14) Babushkin, D. E.; Semikolenova, N. V.; Panchenko, V. N.; Sobolev, A. P.; Zakharov, V. A.; Talsi, E. P. *Macromol. Chem. Phys.* **1997**, *198*, 3845−54.

(15) Zakharov, V. A.; Talsj, E. P.; Zakharov, I. I.; Babushkin, D. E.; Semikolenova, N. V. *Kinet. Catal.* **1999**, *40*, 836−50.

10.1021/ja011092a CCC: $20.00

with trimethylaluminum ($\delta = 153$ ppm; fwhm = 850 Hz).[1,13,15] However, other studies determined the chemical shift of MAO to be located around 50 ppm[16] or at both 60 and 153 ppm.[14] MAO has multiple equilibria in solution along with complexation reactions with trimethylaluminum.[17−18] Solution-state $^{27}$Al NMR shows mostly 4-coordinate aluminum but cannot directly determine the coordination of the aluminum sites in pristine MAO due to the interconversion of various MAO oligomers. As yet, there are no reports of the solid-state spectra of pristine MAO; partially decomposed samples show 3-, 4-, 5-, and 6-coordinate aluminum sites on the basis of chemical shifts for $AlO_n$ coordination. Two different formula units for MAO have been proposed, both with $CH_3$ to Al ratios of approximately 1.5:1, $[-(CH_3)_{1.4-1.5}AlO_{0.8-0.75}-]$[4] and $[Al_4O_3(CH_3)_6]_4$.[19] The average molecular weight in toluene is 1100,[3] in agreement with some proposed cage structures.[3,4] The proposed MAO cage structures have never been prepared and isolated due to their high reactivity, a fact which complicates the further characterization of MAO. Recently, a number of cage structures have been proposed and examined through energies of formation derived from molecular orbital calculations.[6]

Traditionally, solid-state $^{27}$Al MAS NMR means high-field, magic-angle-spinning NMR. The spectra yield three NMR parameters: isotropic chemical shift, $\delta_{iso}$; quadrupole coupling constant, $C_q = e^2q_{zz}Q/h$; asymmetry parameter, $\eta$. The latter two, $C_q$ and $\eta$, are parameters of the electric field gradient tensor (EFG), a ground-state property of the charge distribution near an aluminum site. However, a successful $^{27}$Al MAS NMR experiment requires a combination of Larmor frequency ($\nu_L$), MAS spin rate ($\nu_r$), $C_q$, and $\eta$ which lead to a line width less than the spin rate.[20] They determined a formula for the field and spinning conditions necessary to acquire a distortionless centerband:

$$C_q^2\left(1+\frac{\eta}{6}\right)^2 \lesssim 112\nu_L\nu_R I^2\frac{2I-1}{9\left(I+\frac{3}{2}\right)}$$

Of course, sample quality must be maintained. However, as shown in Figure 1, the aluminum sites in MAO yield an apparently beautiful spectrum for the slightly decomposed MAO but have such large $C_q$ values for the pristine sample that undistorted spectra are almost inaccessible with current MAS NMR techniques.

At this point, the spin rate and magnetic field necessary to acquire an $^{27}$Al MAS NMR spectrum of MAO is unknown. We need an estimate of the $C_q$ and $\eta$ values for MAO. For the $S = 5/2$ $^{27}$Al nucleus, the line-narrowing capability of MAS NMR is shown in Figure 2; a state-of-the-art 833 MHz ($^1$H at 19.6 T) NMR with a 25 kHz MAS probe can access aluminum sites with $C_q$ values up to 18 MHz ($\eta = 1$).

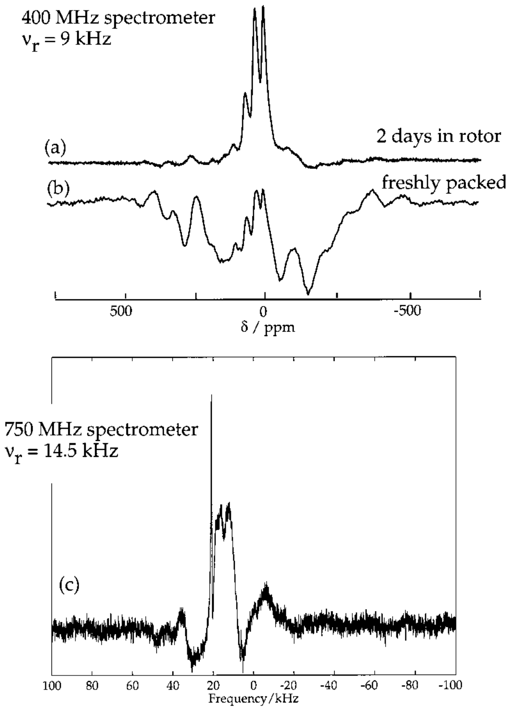

**Figure 1.** MAO's extreme reactivity with air can easily lead to false results. For MAO (solid) spectra similar to (a) have been considered as valid, though more attention to sample handling yields a considerably different spectrum, (b). The distorted appearance (poor signal-to-noise) of (b) means the spin rate and NMR magnetic field are both too small to line-narrow the $^{27}$Al resonances causing most aluminum signal to remain "invisible"; see Figure 2. The magnitude of the $^{27}$Al quadrupolar interaction leads to a requirement for high magnetic fields and high MAS spin rates. (c) However, even $\nu_r = 14.5$ kHz and $B_o = 19.6$ T (750 MHz, $^1$H) is insufficient to acquire an undistorted spectrum.

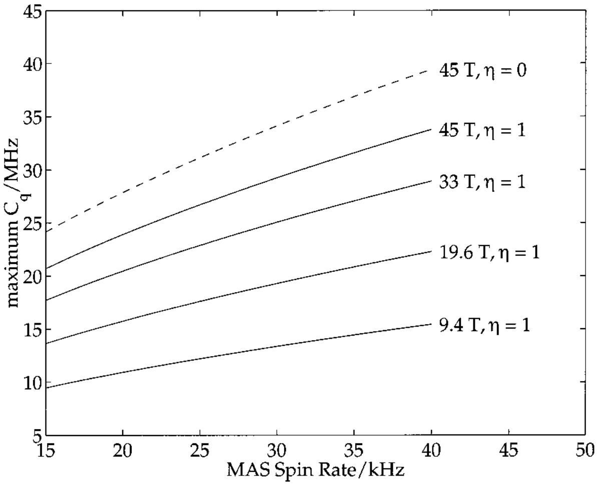

**Figure 2.** Calculated maximum $C_q$ and $\eta$ values for which a line-narrowed $^{27}$Al spectrum can be obtained as a function of MAS spin rate and magnetic field. On the basis of $^1$H NMR, these fields correspond to 400 MHz, 833 MHz, 1.4 GHz, and 1.9 GHz, respectively ($\gamma(^1H)/\gamma(^{27}Al) = 3.8378$). Herein, MAS spin rates range from 9 to 20 kHz and magnetic fields range from 9.4 to 24 T, though experiments at the highest fields are nonspinning experiments.

In this work, we pursue a two-prong investigation. First, we seek a reliable $^{27}$Al NMR spectrum of MAO. Second, molecular aluminum clusters[21] analogous to proposed MAO units are studied, both experimentally with $^{27}$Al NMR and with molecular orbital calculations to generate $^{27}$Al NMR parameters. Then, the validated MO methods are used to predict $^{27}$Al NMR spectra for proposed structures, and calculated spectra are compared with the best available experimental spectra. There are several alternatives to MAS NMR: MQMAS enhances resolution by reducing the quadrupolar broadening in the isotropic dimension and provides correlations between chemical shift and $C_q$ yet is

---

[16] Simeral, L. S.; Zens, T.; Finnegan, J. *Appl. Spectrosc.* **1993**, *47*, 1954−6.

[17] Pasynkiewicz, S. *Polyhedron* **1990**, *9*, 429−53.

[18] Resconi, L.; Bossi, S.; Abis, L. *Macromolecules* **1990**, *23*, 4489−91.

[19] von Lacroix, K.; Heitmann, B.; Sinn, H. *Macromol. Symp.* **1995**, *97*, 137−42.

[20] Skibsted, J.; Bildsøe, H.; Jakobsen, H. J. *J. Magn. Reson.* **1991**, *92*, 669−76.

[21] Schauer, S. J.; Robinson, G. H. *J. Coord. Chem.* **1993**, *30*, 197−214.

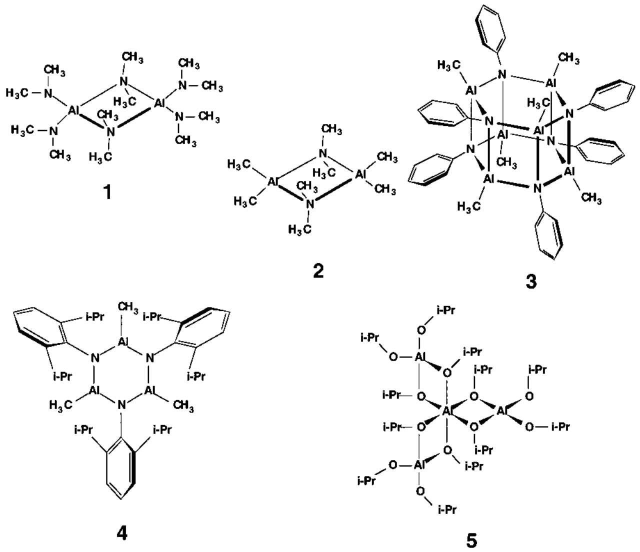

**Figure 3.** (Aminato)- and (propanolato)aluminum clusters. All of these structures can be visualized as oligomers; i.e., **1** and **2** are dimers of $Al(NMe_2)_3$ and $Me_2Al(NMe_2)$, respectively. Other clusters are **3**, hexamer of MeAlN(phenyl), **4**, trimer of MeAlN(2,6-bis(1-methylethyl)phenyl), and **5**, tetramer of tris(isopropoxo)aluminum.

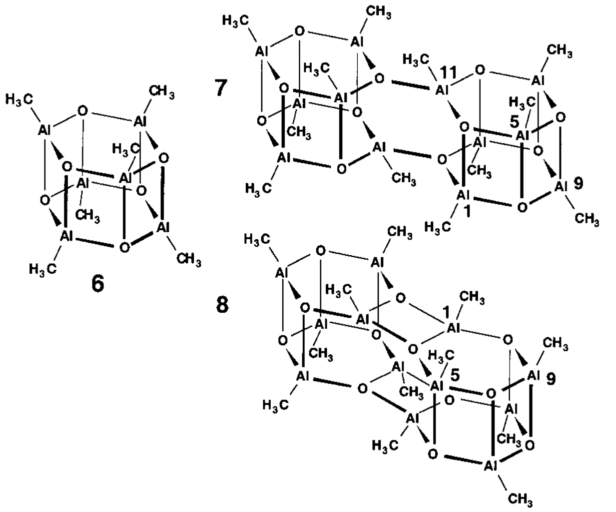

**Figure 4.** Model structures for principal MAO components. All of these structures can be visualized as oligomers: **6**, hexamer of MeAlO, a $D_{3d}$-symmetry oxane cage structure; **7**, a $C_{2h}$ edge-bridged dimer of **6**; **8**, a $D_2$ face-bridged dimer of **6**.

limited by spin-rate and $B_\mathrm{o}$ to the same extent as MAS NMR.[22−26] Zero-magnetic field methods such as nuclear quadrupole resonance are effective for $^{27}$Al in molecular species[27,28] but are difficult to apply to systems with a distribution of resonances and sites.[29] Recently, methods designed to access the full, quadrupolar-broadened line-shape have returned.[30−33] In these methods, either the field or the frequency is adjusted as the spectrum is acquired piecewise over an unlimited spectral range.

The main parameters in $^{27}$Al NMR spectroscopy are the isotropic chemical shift, $\delta_\mathrm{iso}$, and the parameters from the electric field gradient tensor, $C_\mathrm{q}$ and $\eta$. For small- to medium-sized clusters, all can be calculated with good accuracy. Recently, we have calculated $^{27}$Al EFG tensor components for the $Al_2SiO_5$ polymorph andalusite and $^{81}$Br $C_\mathrm{q}$ and $\eta$ values for brominated aromatics (flame-retardants).[34,35] In the best cases, calculated $^{27}$Al EFG tensor orientations are within 2° of experiment, and the $^{81}$Br $C_\mathrm{q}$ values compared well to an experimentally noted trend with aromatic ring substitutent Hammett $\sigma$ values. For the structures shown in Figures 3 and 4, reliable $^{27}$Al $C_\mathrm{q}$ and $\eta$ values require optimized structures and triple-$\zeta$ basis sets, though useful results can be obtained with less extensive basis sets. Inclusion of correlation effects, through the use of density functional theory, makes only a small change in the values of $^{27}$Al $C_\mathrm{q}$ and $\eta$. The importance of calculated $^{27}$Al $C_\mathrm{q}$ and $\eta$ values for this work is large, as the aluminoxanes are highly reactive and model compounds difficult to obtain.

## Experiment Section

**Synthesis. Aminato Aluminum Clusters.** The (aminato)aluminum clusters were typically prepared by the low-temperature addition of an amine to a toluene solution of trimethylaluminum or other alane: 1, bis[$\mu$-(dimethylaminato)]tetrakis(*N*-methylmethanaminato)-dialuminum (32093-39-3);[36] 2, tetramethylbis[$\mu$-(*N*-methylmethanaminato)]dialuminum (22450-81-3);[37−38] 3, hexakis[$\mu^3$-(benzenaminato)]-hexamethylhexaaluminum (100494-82-4);[39] 4, tris[$\mu$-[2,6-bis(1-methylethyl)benzenaminato]]trimethyltricycloaluminum (117960-70-0).[40]

**(Propanolato)tetraaluminum**. This was purchased from Aldrich and used as received. The hexakis[$\mu$-(2-propanolato)]hexakis(2-propanolato)tetraaluminum (25443-56-5) structure was reported by Folting et al.[41]

**MAO**. Solid samples of MAO (from Albemarle Corporation) were obtained by evaporation of 30% MAO in toluene to dryness under high vacuum. After drying, the solids were held under vacuum for about 1 h. Solid dry samples of MAO (gel) were prepared by allowing high activity 30% MAO in toluene to stand in a closed container in an inert atmosphere at room temperature for 6−12 months. Solvent was decanted from the gel several times following stirring and settling. Samples of the wet gel were then dried under high vacuum for about 1 h.

MAO(solid) and MAO(gel) were checked for air exposure prior to solid-state NMR experiments to ensure pristine samples for analysis. The solid samples were dissolved in $C_6D_6$ or in THF-$d_8$, and the proton

---

[22] Medek, A.; Harwood: J. S.; Frydman, L. *J. Am. Chem. Soc.* **1995**, *117*, 12779−87.

[23] Rocha, J. *J. Chem. Soc., Chem. Commun.* **1998**, 2489−90.

[24] Alemany, L. B.; Steuernagel, S.; Amoureux, J.-P.; Callender, R. L.; Barron, A. R. *Solid State Nucl. Magn. Reson.* **1999**, *14*, 1−18.

[25] Bodart, P. R.; Parmentier, J.; Harris, R. K.; Thompson, D. P. *J. Phys. Chem. Solids* **1999**, *60*, 223−8.

[26] Lee, S. K.; Stebbins, J. F. *J. Phys. Chem. B* **2000**, *104*, 4091−100.

[27] Dewar, M. J. S.; Patterson, D. B.; Simpson, W. I. *J. Am. Chem. Soc.* **1971**, *93*, 1030−2.

[28] Dewar, M. J. S.; Patterson, D. B.; Simpson, W. I. *J. Chem. Soc., Dalton Trans.* **1973**, 2381−90.

[29] Mrse, A. A.; Lee, Y.; Bryant, P. L.; Fronczek, F. R.; Butler, L. G.; Simeral, L. S. *Chem. Mater.* **1998**, *10*, 1291−300.

[30] Poplett, I. J. F.; Smith, M. E. *Solid State NMR* **1998**, *11*, 211−4.

[31] Wu, X.; Juban, E. A.; Butler, L. G. *Chem. Phys. Lett.* **1994**, *221*, 65−7.

[32] Clark, W. G.; Hanson, M. E.; Lefloch, F.; Segransan, P. *Rev. Sci. Instrum.* **1995**, *66*, 2453−64.

[33] Bryant, P. L.; Butler, L. G.; Reyes, A. P.; Kuhns, P. *Solid State NMR* **2000**, *16*, 63−7.

[34] Bryant, P. L.; Harwell, C. R.; Wu, X.; Fronczek, F. R.; Hall, R. W.; Butler, L. G. *J. Phys. Chem. A* **1999**, *103*, 5246−52.

[35] Harwell, C. R.; Shelby, A. I.; Mrse, A. A.; Butler, L. G.; Hall, R. W. *J. Phys. Chem. A*, **1999**, *103*, 8088−92.

[36] Waggoner, K. M.; Olmstead, M. M.; Power, P. P. *Polyhedron* **1990**, *9*, 257−63.

[37] Thomas, C. J.; Krannich, L. K.; Watkins, C. L. *Polyhedron* **1993**, *12*, 389−99.

[38] McLaughlin, G. M.; Sim, G. A.; Smith, J. D. *J. Chem. Soc., Dalton Trans.* **1972**, 2197−203.

[39] Al-Wassil, A. A. I.; Hitchcock, P. B.; Sarisaban, S.; Smith, J. D.; Wilson, C. L. *J. Chem. Soc., Dalton Trans.* **1985**, 1929−34.

[40] Evans, W. J.; Ansari, M. A.; Ziller, J. W.; Khan, S. I. *Inorg. Chem.* **1996**, *35*, 5435−44.

[41] Folting, K.; Streib, W. E.; Caulton, K. G.; O. Poncelet; Hubert-Pfalzgraf, L. G. *Polyhedron* **1991**, *10*.

NMR spectra were obtained at 400 MHz. The high signal-to-noise spectra were examined for alkoxide (from any air exposure) resonances in the 3−4 ppm region. Except as noted the area of the alkoxide, if observed at all, was less than about 1% of the total MAO methyl group resonances.

**NMR Spectroscopy. MAS NMR.** All rotors were loaded in argon- or nitrogen-filled gloveboxes and transported to the NMR in capped vials. At the NHMFL, a very narrow bore Magnex 19.6 T (833 MHz, $^1$H) with a Bruker Avance console was used. The 2.5 mm $ZrO_2$ rotors and tight fitting Kel-F caps were spun with air to 20 kHz in a Samoson-style probe. Experiment times were always less than 30 min. All 35 kHz $^{27}$Al MAS NMR data were spun in air using 2.0 mm $ZrO_2$ rotors and Kel-F caps. At EMSL/PNNL, a narrow-bore 17.6 T (750 MHz, $^1$H) magnet was used with a Varian console. The 5 mm $Si_3N_4$ rotors were fitted with O-ring sealed caps and spun with $N_2$ to 14.5 kHz in a Jakobsen-style probe. Chemical shifts were set via $Al(NO_3)_3$ solution to 0 ppm or with $\alpha$-$Al_2O_3$ to 18.8 ppm.[42]

To assess the concern of air reactivity, spectra were acquired at 9.4 T (400 MHz, $^1$H) over 24 h of spinning with air at 9 kHz in a 5 mm $ZrO_2$ rotor fitted with a Kel-F cap having a pressure relief pinhole. The MAO air decomposition peaks are three narrow resonances at shifts corresponding to 4-, 5-, and 6-coordinate $AlO_x$ sites, 67, 35, and 8.9 ppm, respectively.[43,44] Hence, aluminum sites with $C_q < 10$ MHz are attributed to decomposition products. No such sites were found in the work done at 17.6 T (O-ring sealed rotor) or at 19.6 T (tight fitting Kel-F cap and <30 min experiment time), with one exception as noted in figure caption. In one overnight run of MAO(gel) at 35 kHz, the Kel-F caps sealed the 2 mm rotor quite tightly and no decomposition was seen.

**Frequency-Stepped NMR**. The frequency-stepped NMR was done on a Chemagnetics Infinity 400 MHz with static (nonspinning) samples in a 5 mm, high-power, low-$Q$[25] probe with low aluminum background and 5.5 $\mu$s recovery time. Pulse power was set with 1 M $Al(NO_3)_3$ to give a 2.75 $\mu$s 90° pulse. For solid samples, the Hahn echo pulse sequence is used with $90_{x-}\tau_1-180_y\angle\tau_2-$acq with typical settings of 0.95 and 1.90 $\mu$s pulses and delays of 5.07 and 5.55 $\mu$s. The echo is acquired with a dwell of 0.4 $\mu$s, data length of 1 k, pulse delay of 5 s, and an accumulation of 1000−4000 transients. The center frequency of the 33 different frequency settings was 104.242 997 MHz, which corresponds to an $^{27}$Al NMR chemical shift of 0 ppm. The frequency increment between settings was 40 kHz, and the 17th and center frequency setting corresponds to an $^{27}$Al NMR chemical shift of 0 ppm. The scan across frequency settings was done in a semiautomatic manner with manual probe retuning, based on minimization of reflected power, at every third frequency setting.

A Matlab program was used to process the NMR data. The signal-averaged echoes are recorded then frequency shifted to a common frequency by the multiplication of the NMR signal, $S_i(t)$, by

$$S(t) = \sum_i S_i(t) \exp\{-2i\pi\Delta f_i[t - t_o]\} \tag{1}$$

where $t_j$ is the time domain axis and $\Delta f_i$ is the frequency difference between the center frequency (0 ppm) and the fixed frequency for each of the 33 echoes. The shifted echoes are Fourier transformed, a magnitude calculation is performed, and then the echoes are summed to produce the final frequency stepped spectrum.

**Field-Swept NMR**. A MAO(gel) spectrum was acquired at 77 K with a Hahn echo sequence of $90_{x-}\tau_{1-}180_{y-}\tau_2-$acq with 3.5 and 7 $\mu$s pulses and delays of 115 and 1 $\mu$s. The echo was acquired with a dwell of 1 $\mu$s, data length of 1 k, pulse delay of 0.5 s, and an accumulation of 32 transients. The spectrometer frequency was constant at 254 MHz. The scan across field settings from 22.9 to 23 T was done with a field increment of 2 mT, which is much smaller than the spectrometer bandwidth; a field settling time of 4 s was used prior to each NMR acquisition.

A LabView program was used to process in near-real time the field-swept NMR data.[33] Data processing consists of offset correction for a dc signal, trapezoidal filtering about the echo, and interpolation of the echo onto a ×2 or ×4 finer time axis. The last step increases the apparent spectrometer bandwidth from 1 to 2 or 4 MHz. Then, the echoes are frequency shifted to a common magnetic field by the phase shifting of the original time domain signal, $S_i(t)$. The resulting expression is summed to give

$$S(t) = \sum_i S_i(t) \exp\{-2i\pi\gamma\Delta B_i[t - t_o]\} \tag{2}$$

where $\Delta B_i$ is the difference in magnetic field from the assigned center of the final spectrum to the magnetic field used to acquire the echo.[32] The parameter $t_o$ is the position of the echo maximum in the time domain.

Most frequency-stepped, field-swept, and MAS NMR spectra were fitted to $S = 5/2$ quadrupolar powder patterns with a nonlinear least squares routine. However, in some cases, especially for frequency-stepped NMR with two aluminum sites, convergence could not be achieved. In those cases, the singularities of the $S = 5/2$ powder pattern were used to generate a best fit by eye.

**EFG Tensor Calculations**. Calculations were performed on IBM RS/6000 workstations and on a 20-node Beowulf cluster. Calculations were performed at the RHF level using GAMESS[45] and at the DFT level (becke31yp) using GAUSSIAN-9x.[46] With the exception of the dimeric cages, the procedure we followed was (a) start with the crystal structure coordinates, (b) manually truncate (if necessary), and (c) symmetrize the structure using Jaguar.[47] All geometries were then optimized for energy and the reported EFG parameters are from the optimized structures. The final geometry for an RHF optimization was used as the initial geometry for the DFT optimization. The final geometry for a given basis set was used as the starting geometry for the next larger basis set. The basis sets used in this progression were STO-3G, cc-pVDZ, and cc-pVTZ.[48] For the dimeric cages, for which no crystal structures exist, we used the optimized $D_{3d}$ structure to manually construct the model cages for a particular structure and then performed a RHF calculation using the cc-pVDZ basis set. Computational limitations prevented DFT and larger basis set calculations on these structures. However, the use of RHF and cc-pVDZ only was justified (see below) by the small differences between RHF/cc-pVDZ and DFT/cc-pVTZ calculations for a model MAO compound.

## Results and Discussion

In this project, several different NMR techniques are evaluated, EFG calculations validated, and both NMR and calculations applied to a variety of organometallic aluminum complexes, including MAO. The results of the presentation will

---

[42] Vosegaard, T.; Jakobsen, H. J. *J. Magn. Reson.* **1997**, *128*, 135−7.

[43] Cruickshank, M. C.; Glasser, L. S. D.; Barri, S. A. I.; Poplett, I. J. F. *J. Chem. Soc., Chem. Commun.* **1986**, 23−4.

[44] Freude, D.; Haase, J. In *NMR Basic Principles and Progress*; Diehl, P. F., E., Günther, H., Kosfeld, R., Seelig, J., Eds.; Springer-Verlag: Berlin, 1993; Vol. 29, pp 1−90.

[45] Schmidt, M. W.; Baldridge, K. K.; Boatz, J. A.; Elbert, S. T.; Gordon, M. S.; Jensen, J. H.; Koseki, S.; Matsunaga, N.; Nguyen, K. A.; Su, S. J.; Windus, T. L.; Dupuis, M.; Montgomery, J. A.; Schmidt, M. W.; Baldridge, K. K.; Boatz, J. A.; Elbert, S. T.; Gordon, M. S.; Jensen, J. H.; Koseki, S.; Matsunaga, N.; Nguyen, K. A.; Su, S. J.; Windus, T. L.; Dupuis, M.; Montgomery, J. A. *GAMESS*, version 31 Oct 1996; Iowa State University: Ames, IA, 1993.

[46] Frisch, M. J.; Trucks, G. W.; Schlegel, H. B.; Gill, P. M. W.; Johnson, B. G.; Wong, M. W.; Foresman, J. B.; Robb, M. A.; Head-Gordon, M.; Replogle, E. S.; Gomperts, R.; Andres, J. L.; Raghavachari, K.; Binkley, J. S.; Gonzalez, C.; Martin, R. L.; Fox, D. J.; Defrees, D. J.; Baker, J.; Stewart, J. J. P.; Pople, J. A. *Gaussian 92/DFT*, revision F.4; Gaussian, Inc.: Pittsburgh, PA, 1993.

[47] *Jaguar*, Jaguar 3.5; Schrödinger, Inc.: Portland, OR, 1998.

[48] *EMSL_Gaussian_basis_set*, EMSL Gaussian basis set order form: http://www.emsl.pnl.gov: 2080/forms/basisform.html. Basis sets were obtained from the Extensible Computational Chemistry Environment Basis Set Database, version 1.0, as developed and distributed by the Molecular Science Computing Facility, Environmental and Molecular Sciences Laboratory, which is part of the Pacific Northwest Laboratory, P.O. Box 999, Richland, WA 99352, and funded by the U.S. Department of Energy. The Pacific Northwest Laboratory is a multiprogram laboratory operated by Battelle Memorial Institute for the U.S. Department of Energy under Contract DE-AC06-76RLO 1830. Contact David Feller, Karen Schuchardt, or Don Jones for further information.

**Table 1.** $^{27}$Al NMR Parameters for (Aminato)- and (Propanolato) aluminum Clusters

| | experiment | | | ab initio MO calculation[a] | | |
|---|---|---|---|---|---|---|
| compd | $\delta_{iso}$/ppm | $C_q$/MHz | $\eta$ | $C_q$/MHz | $\eta$ | structure calcd |
| **1,** $[((Me_2N)_2Al)(NMe_2)]_2$ (4-member ring, 4-coord, $AlN_4$) | 110(20) | 12.2(5) | 0.8(1) | 14.163 | 0.76 | $[Al(NMe_2)_3]_2$ |
| **2,** $[(Me_2Al)(NMe_2)]_2$ (4-member ring, 4-coord, $AlC_2N_2$) | 170(20) | 15.8(1) | 1.0(1) | −19.082 | 0.92 | $[(Me_2Al)(NMe_2)]_2$ |
| **3,** $[(MeAl)(NC_6H_5)]_6$ (cage, 4-coord, $AlCN_3$) | 160(20) | 17.51(3) | 0.52(5) | −18.214 | 0.62 | $[(MeAl)(NMe)]_6$ |
| **4,** $[(MeAl)(N(2,6\text{-}i\text{-}PrC_6H_3)\ )]_3$ (6-member ring, 3-coord, $AlCN_2$) | 170(20) | 37(1) | 0.0(5) | 39.950 | 0.01 | $[(MeAl)(NMe)]_3$ |
| **5,** $Al[(\mu\text{-}O^iPr)_2Al(O^iPr)_2]_3$ | | | | | | $Al[(\mu\text{-}O^iPr)_2Al\ (O^iPr)_2]_3$ |
| 6-coord, $AlO_6$ | | <2 | | 0.293 | 0 | |
| 4-coord, $AlO_4$ | 65(1) | 12.31(2) | 0.14(2) | 14.159 | 0.11 | |

[a] Calculated from fully optimized geometries using RHF with correlation consistent polarized cc-pVTZ basis sets.

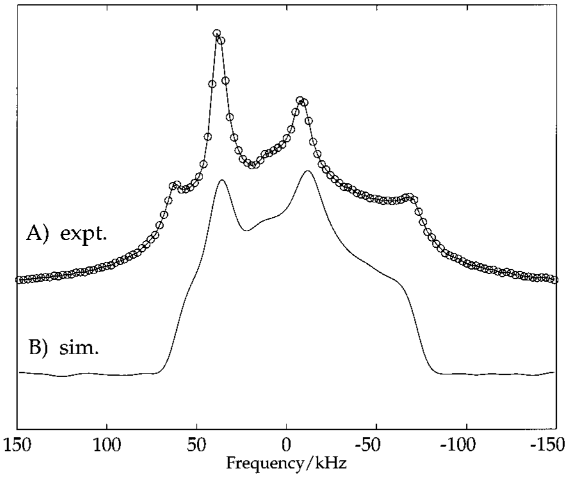

**Figure 5.** Frequency-stepped NMR of (aminato)hexaluminum cluster (A), **3**, at 9.4 T. The spectrum is a sum of 33 subspectra, each acquired at 40 kHz intervals across the $^{27}$Al resonance. The complete spectrum acquired in 46 h. $C_q$, $\eta$, and $\delta_{iso}$ are obtained by nonlinear least-squares fit (B).

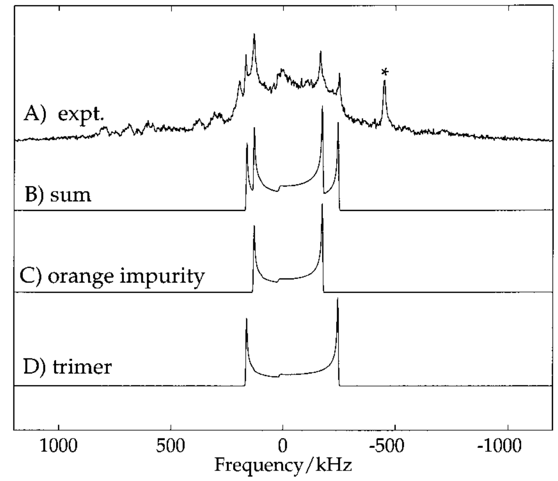

**Figure 6.** Frequency-stepped NMR spectrum (A) of planar, 3-coordinate aluminum in an (aminato)trialuminum ring, **4**. The spectrum is fitted with a sum (B) of two $^{27}$Al powder patterns, (C) an orange impurity with $C_q = 32$ MHz, $\eta = 0$, and (D) the trimer with $C_q = 37$ MHz, $\eta = 0$. The wide spectral range for $^{27}$Al NMR at 9.4 T overlaps the FM radio band. The asterisk marks a radio station signal.

follow this order: an overview of the three NMR techniques used herein; a presentation of the NMR experiments and EFG calculations for aminato complexes (these results verify the MAS NMR limits plotted in Figure 2 and show the accuracy of EFG calculations for large organometallic aluminum clusters); an examination of NMR and EFG calculations of a molecular Al−O complex, a (propanolato)tetraaluminum complex, which shows that the techniques developed for Al−N complexes are applicable to Al−O complexes. Last, the NMR results for MAO solid and gel are compared with three plausible cage structures.

**NMR Techniques**. Three different NMR techniques are used in this work. When possible, high-speed, high-field MAS NMR is used, although, as noted in Figure 1, the MAO sample is difficult to study with currently available fields and spin rates. As shown in Figure 2, useful $^{27}$Al MAS NMR spectra can be obtained for small to moderate $C_q$ values. However, $C_q$ values are known to range up to 45 MHz for 3-coordinate aluminum sites,[28] greatly exceeding the present capabilities of high-speed, high-field MAS NMR. For large $C_q$ sites, two wide-spectral width methods are used with static (nonspinning) samples: Frequency-stepped NMR is used with persistent superconducting magnets and field-swept NMR is used with powered magnets, either superconducting or resistive. Of these, field-swept NMR is preferred for two reasons: Acquisition of spectra at several different fields aids analysis; the shape of the quadrupolar powder pattern is field dependent. Also, the constant spectrometer frequency during a swept simplifies data processing. Still, frequency-stepped NMR is found to be reliable for materials with a single aluminum site of moderate to large $C_q$ value and this method was used in the exploratory phase of this project.

**Aminato Complexes**. Four (aminato)aluminum complexes were studied with frequency-stepped NMR and MO calculations; the results are summarized in Table 1. The experimental $C_q$ and $\eta$ values follow expected trends and are well modeled with EFG calculations. The smallest value for $C_q$ is found for a nominally tetrahedral $AlN_4$ site in **1**, though the ring strain, ∠N−Al−N = 88.2°, associated with the four-membered ring leads to a significant $C_q$ value of 12.2 MHz. Of course, a perfectly tetrahedral $AlN_4$ site would have $C_q = 0$ MHz. Compound **2** has a very similar geometry, again a strained four-membered ring, yet the change in coordination to $AlN_2C_2$ causes $C_q$ to increase, as expected, to 15.8 MHz. For both **1** and **2**, the magnitude of the calculated $C_q$ values are somewhat larger than experiment, by 2−3 MHz, while the asymmetry parameters are within 0.1.

An (aminato)hexaaluminum cluster[39] with $AlC_3N$ sites, **3**, was studied by frequency-stepped NMR and MO calculations. The spectrum is shown in Figure 5. The singularities of the $S = 5/2$ powder pattern match well with those of a best-fit simulated NMR spectrum used to extract the $C_q$ and $\eta$ values. The aluminum site is 4-coordinate but has a surprisingly large $C_q$ value of 17.5 MHz. The large quadrupole coupling constant is attributed to the two strained four-membered rings in which the aluminum site is contained. At 17.5 MHz, this $C_q$ nears the upper limit of MAS NMR spectroscopy (see Figure 2), with a spin rate of 25 kHz at 19.6 T needed for $C_q$ =17.5, $\eta = 1$. The utility of frequency-stepped NMR is apparent, though overlapping powder patterns remain problematic. The single aluminum site in **3** is easily analyzed. The results of the MO calculation

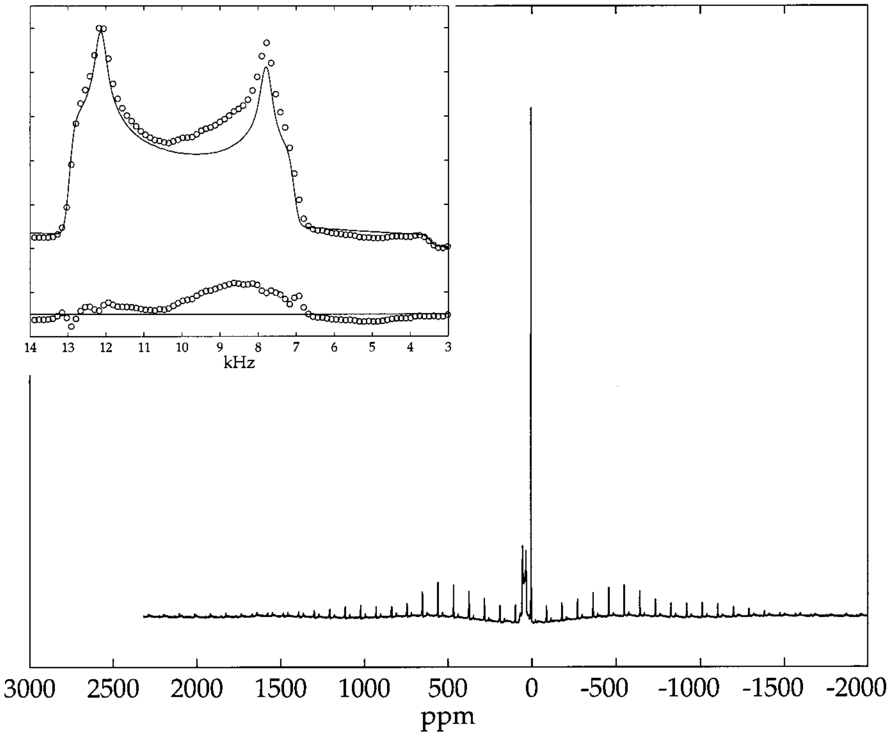

**Figure 7.** MAS NMR of the (propanolato)tetraaluminum complex, **5**. Spin rate = 20 kHz, and $B_o$ = 19.6 T (833 MHz $^1$H). The $C_q$ and $\eta$ values of the $AlO_4$ site were determined with nonlinear least-squares fits to the MAS narrowed central transition (insert).

**Table 2.** Calculated $^{27}$Al NMR Parameters for Aluminoxane Cage and Two Dimers

| compd | site | $C_q$/MHz | $\eta$ | method | basis set |
|---|---|---|---|---|---|
| **6,** [(MeAl)(OMe) ]$_6$ | 1 | −21.430 | 0.646 | rhf | cc-pVDZ |
| (cage, 4-coord, $AlO_3C$) | 1 | −24.062 | 0.751 | rhf | cc-pVTZ |
| | 1 | −18.91 | 0.618 | b3lyp | cc-pVDZ |
| | 1 | −23.71 | 0.742 | b3lyp | cc-pVTZ |
| **7,** [(MeAl)(OMe) ]$_{12}$ | 1 | −19.5 | 0.47 | rhf | cc-pVDZ |
| edge-bridged dimer of **6** | 5 | −22.1 | 0.54 | rhf | cc-pVDZ |
| | 9 | −22.1 | 0.63 | rhf | cc-pVDZ |
| | 11 | −15.4 | 0.20 | rhf | cc-pVDZ |
| **8**, [(MeAl)(OMe) ]$_{12}$ | 1 | −16.49 | 0.906 | rhf | cc-pVDZ |
| face-bridged dimer of **6** | 5 | −18.04 | 0.614 | rhf | cc-pVDZ |
| | 9 | −22.57 | 0.407 | rhf | cc-pVDZ |

also yields a large $C_q$ value of −18.214 MHz (see Table 1), though the calculation is performed for an *N*-methyl rather than an *N*-phenyl complex so as to reduce computational requirements to a manageable level.

The largest $C_q$ found in this work, 37 MHz, is associated with the planar, 3-coordinate aluminum site of **4**, an $AlN_2C$ site.[49] The calculated $C_q$ is 39.95 MHz, and like the experiment, the asymmetry parameter is near zero. Interestingly, the frequency-stepped NMR spectrum of **3** is relatively easy to obtain (Figure 6), although compromised by an orange decomposition product tentatively attributed to coupling reactions at the aromatic ring leading to another 3-coordinated aluminum site; the parameters for the decomposition product are $C_q$ = 32 MHz, $\eta = 0$.

At 37 MHz, the (aminato)trialuminum ring, **4**, has one of the largest known aluminum quadrupole coupling constants and the largest measured yet with NMR. NQR was successful for tri-*tert*-butylaluminum at 45.41 MHz[28] and gas-phase microwave spectroscopy is also useful at high $C_q$: AlCN, −37.2225(29);[50] $(CH_3)_3N{-}AlH_2D$, 25.117(16) MHz;[51] $(CH_3)_3Al{-}NH_3$, 28.30(1) MHz.[52] It is important for this work to find NMR methods compatible with large $C_q$ $^{27}$Al systems. We suspect NQR will be difficult or misleading for MAO with its distribution of aluminum sites, much like the exceedingly broad $^{81}$Br NQR lines of the dispersed flame retardants in polystyrene.[29]

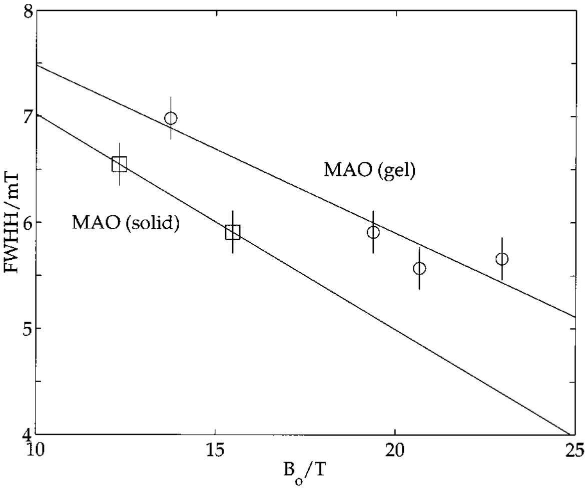

**Figure 8.** Measured line widths as a function of field strength for MAO (solid) (square) and MAO (gel) (circle). On the basis of this observation, MAO(gel) has sites with larger $C_q$ than those of MAO (solid).

**(Propanolato)tetraaluminum Complex**. Some of the techniques developed for the Al−N complexes are now applied to an Al−O complex. The (propanolato)tetraaluminum cluster, **5**, contains one octahedral $AlO_6$ site and three equivalent $AlO_4$ sites. As for the 4-coordinate aminato sites, ring strain at the

---

[49] Waggoner, K. M.; Hope, H.; Power, P. P. *Angew. Chem., Int. Ed. Engl.* **1988**, *100*, 1699−700.

[50] Walker, K. A.; Gerry, M. C. L. *Chem. Phys. Lett.* **1997**, *278*, 9−15.

[51] Warner, H. E.; Wang, Y.; Ward, C.; Gillies, C. W.; Interrante, L. *J. Phys. Chem.* **1994**, *98*, 12215−22.

[52] Müller, J.; Ruschewitz, U.; Indris, O.; Hartwig, H.; Stahl, W. *J. Am. Chem. Soc.* **1999**, *121*, 4647−52.

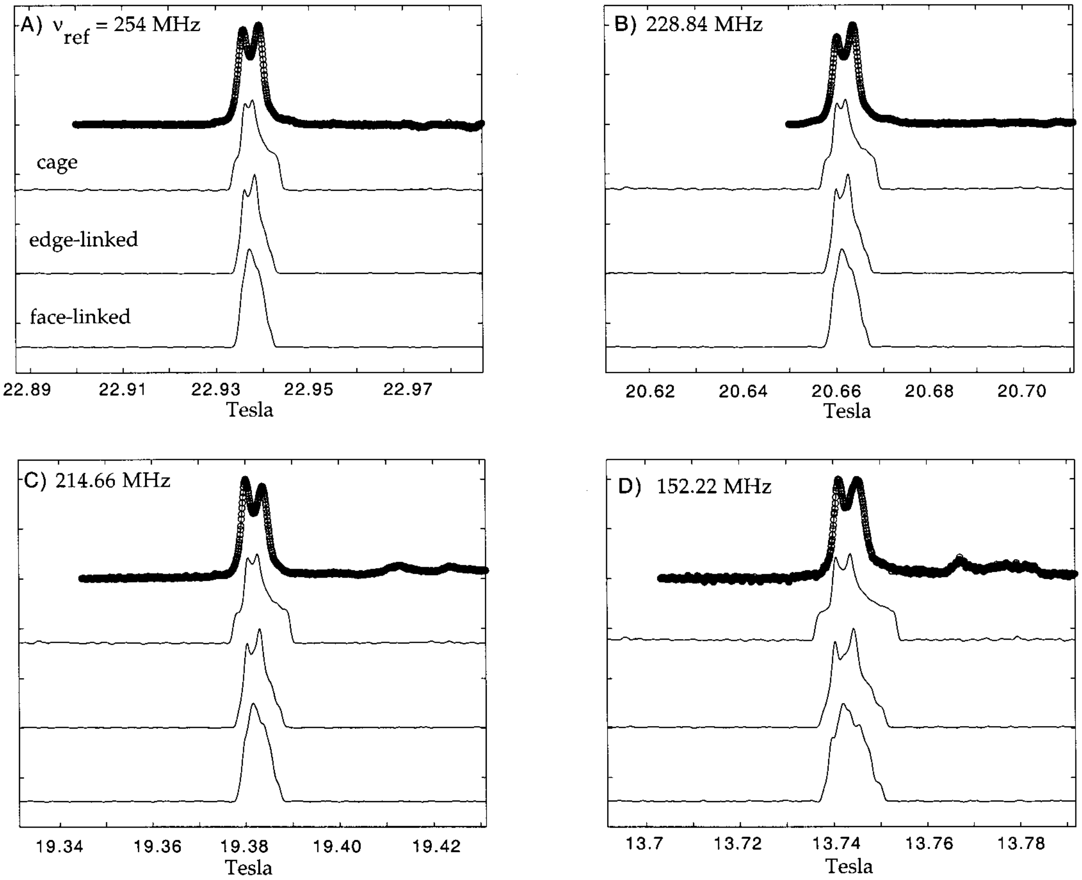

**Figure 9.** Field-swept of MAO gel between 13 and 23 T (top trace). Shown below are predicted spectra for the proposed $D_{3d}$ hexameric cage, **6**, the $C_{2h}$ edge-bridged cage dimer, **7**, and the $D_2$ face-bridged cage dimer, **8**.

$AlO_4$ sites leads to moderate $C_q$ values, as measured with high-speed, high-field MAS NMR, shown in Figure 7, and confirmed with calculations (Table 1). The spinning sideband pattern is seen for both sites, with that of the 5 ppm, $AlO_6$ site extending to ±15 discernible sidebands. The high quality of this $^{27}$Al MAS NMR spectrum demonstrates the clear advantage of MAS NMR for resolution of multiple components, provided $C_q$ is less than the limit shown in Figure 2 for $B_o$ and spin rate available.

The (propanolato)tetraaluminum complex, **5**, was also studied with frequency stepped and field swept NMR. The former was done at 9.4 T and shows two, overlapping $^{27}$Al quadrupolar powder patterns. The field swept NMR spectrum was acquired at 20.8 T, which proved to be so large as to narrow the $^{27}$Al powder patterns such that the singularities were then obscured by other line broadening mechanisms such as the field inhomogeneity of the resistive magnets.

At this point, four (aminato)- and one (propanolato)aluminum complexes have been studied via three different $^{27}$Al NMR methods. In all cases, $^{27}$Al $C_q$ and $\eta$ values are obtained for the one or two sites present in the complexes. The chemical shift values are consistent with previous literature values of the same or similar compounds.[36,49,53−56] In addition, we have found very good accuracy for the $C_q$ and $\eta$ values from the EFG calculations of respective complexes or truncated versions of the same (Table 1). A critical feature of the calculations is geometrical optimization of the calculated structure. Similar structural dependency was noted for calculated $^{81}$Br $C_q$ values in brominated aromatics and BrCl dimer.[35,57] With geometry optimization and triple-$\zeta$ basis sets, calculated $C_q$ values are generally within 3 MHz and $\eta$ is within 0.1. While all calculated results reported in Table 1 are from RHF/cc-pVTZ calculations, we found that RHF with double-$\zeta$ basis sets gave similar values, provided geometry-optimized structures are used, as can be seen in a study of the hexameric cage, **6**, listed in Table 2.

**MAO Solid and Gel**. Methylaluminoxane is typically prepared in toluene solution. Subsequent solvent removal yields the MAO(solid). Without cold storage, the MAO/toluene solution will gel; removal of excess toluene yields the MAO(gel) studied herein. An initial hypothesis of this work is some discernible difference in the structure at aluminum sites, though as yet, no differences have been found between the two forms with low-field, low-speed MAS NMR.

Initially, the field-swept NMR spectra of MAO(solid) and (gel) are compared by examination of the line-widths, as shown in Figure 8. Over this small change in magnetic field, the line widths do not show the expected inverse dependence upon the square of the magnetic field; this is attributed to multiple aluminum sites. The line widths for MAO(gel) are significantly larger than found for MAO(solid), indicating dominance by sites with larger $C_q$ values. Because of the larger $C_q$ values, MAO(gel) will be a more difficult sample to study via high-field,

---

(53) Benn, R.; Rufinska, A.; Lehmkuhl, h.; Janssen, E.; Krüger, C. *Angew. Chem., Int. Ed. Engl.* **1983**, *22*, 779−80.

(54) Benn, R.; Janssen, E.; Lehmkuhl, H.; Rufinska, A. *J. Organomet. Chem.* **1987**, *333*, 155−68.

(55) Pinkas, J.; Gaul, B.; Verkade, J. G. *J. Am. Chem. Soc.* **1993**, *115*, 3925−31.

(56) Park, J. E.; Bae, B. J.; Kim, Y.; Park, J. T.; Suh, I. H. *Organometallics* **1999**, *18*, 1059−67.

(57) Fowler, P. W.; Legon, A. C.; Peebles, S. A.; Steiner, E. *Chem. Phys. Lett.* **1995**, *238*, 163−7.

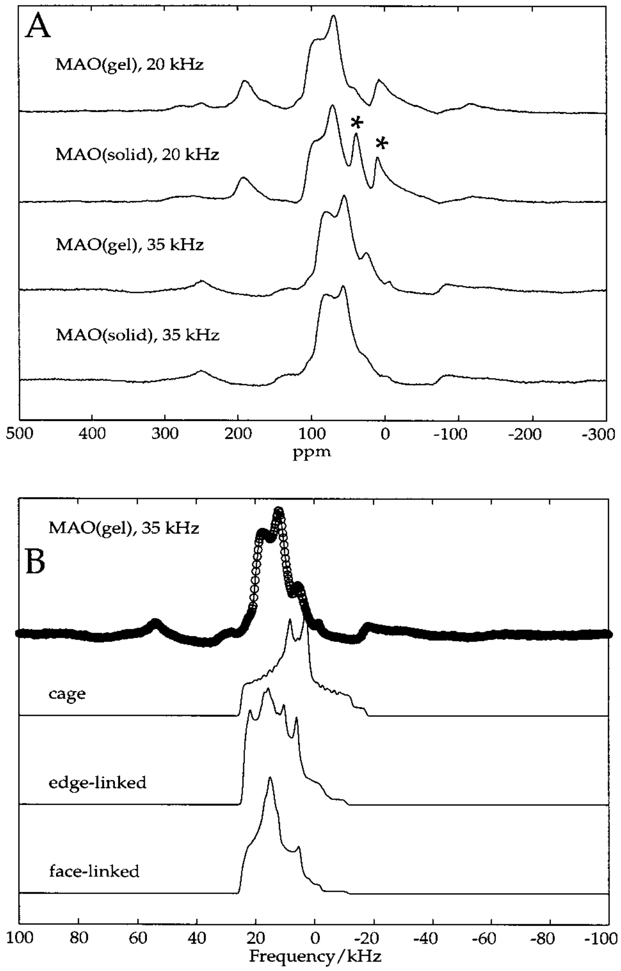

**Figure 10.** High-field, high-speed MAS NMR spectra of MAO(gel) and MAO(solid). (A) Spectra were acquired with an 833 MHz (19.6 T) NMR and 2.5 mm (20 kHz spin rate) and 2.0 mm (35 kHz) rotors. Marked in (A) are two peaks likely associated with air-induced decomposition (*). Note: the spectra acquired at 20 kHz spin rate are chemical shift referenced to $\alpha$-$Al_2O_3$ but the 35 kHz spin rate spectra were not acquired with a chemical shift reference. In (B) are shown the simulated MAS spectra of three plausible structures based on the calculated $C_q$ and $\eta$ values listed in Table 2 and with the assumption of a constant chemical shift for all aluminum sites.

high-speed MAS NMR than MAO(solid). In this section, we present field-swept NMR results and then high-field, high-speed MAS NMR spectra.

The field-swept spectra of MAO(gel) are shown in Figure 9 at four different magnetic field ranges. The purpose of the four different fields is to explore the evolution of the line shape; the highest magnetic field allows better observation of very large $C_q$ sites while the lowest field differentiates between sites of moderate $C_q$ values. Also shown below each experimental spectrum are simulations of line shapes expected for the postulated hexameric cage, **6**, the edge-bridged cage dimer, **7**, and the face-bridged cage dimer, **8**. Line drawings of each structure were shown in Figure 4, and the results of the EFG calculations are given in Table 2. As can be seen in the spectrum acquired around 13.75 T (Figure 9D), the hexameric cage is not a good model for MAO(gel); its calculated $C_q = 23.71$ MHz and $\eta = 0.74$ yield a line shape broader than experimental spectrum. Interesting, the edge-linked cage has the best overall match with the four experimental spectra, both in terms of line shape and line width. The edge-linked cage has four unique sites (Table 2) with $C_q$ ranging from 15.4 to 22.1 MHz.

Three-coordinate aluminum sites are not evident in any of the MAO(gel) field-swept NMR spectra. If present, those sites would have a $C_q \geq 35$ MHz and a powder pattern broader than that of "cage" in Figure 9, which has $C_q = -21.43$ MHz (cc-pVDZ). Also, on the basis of the poorly resolved spectra acquired at 400 MHz (Figure 1), $C_q$ is greater than 10 MHz for all aluminum sites in MAO(solid) and MAO(gel) (spectrum not shown). Therefore, the search for plausible structures is now guided by $|C_q|$ values lying in the range of 10−21 MHz.

High-field, high-speed MAS spectra of MAO(gel) and MAO(solid) are shown in Figure 10. One difference between the apparatus for field-swept NMR and MAS NMR is the protection of the sample from air-induced decomposition; the sample is better protected in the field-swept NMR whereas, in air-spun MAS NMR, the lifetime of a pristine sample is on the order of minutes. At 35 kHz spin rate, the MAO(gel) and (solid) show roughly similar line shapes and widths. Like all of the previous MAS NMR spectra of MAO, the gel and solid are not conclusively shown to be different. Thus, our only evidence in a difference between these two samples is the difference in line widths seen in the field-swept spectra (Figure 8).

Figure 10B shows simulated MAS NMR spectra for the plausible structures, cage **6**, edge-linked cage **7**, and face-linked cage **8**. As in the field-swept comparisons, the cage structure does not match the MAO(gel) spectrum. Interestingly, both the edge-linked and face-linked may be possible components of MAO(gel); the line widths of the simulated are close to the experimental line width, and a combination of these two species may lead to the observed line shape. If, indeed, cage-type structures like **6** are basic units in MAO, then linking of the units is necessary to reach the observed molecular weights. We note that the simulated spectra are not yet corrected for variations of isotropic chemical shifts among the 4 and 3 different sites in **7** and **8**, respectively.

One additional approach to line-narrowing quadrupolar resonances is temperature-induced mobility. The $^{27}$Al MAS NMR spectrum of MAO as acquired at 400 MHz ($^1$H) is essentially unchanged from −80 to 130 °C, both for pristine and MAO after slight air-induced decomposition (see Figure 1a,b). Thus unlinked cage with potentially high mobility appears unlikely.

## Conclusions

Structural characterization of MAO is desired since aluminum site structure is likely closely associated with the catalytic promotion effected by MAO. However, $^{27}$Al NMR spectroscopy is difficult given the large quadrupole coupling constants found thus far for all aluminum sites in the complex mixture that makes up MAO. This study reports NMR spectra of discrete (aminato)- and (propanolato)aluminum clusters with structural types likely to be found in MAO. In the course of the work, three $^{27}$Al NMR methods are evaluated: high-field MAS NMR; frequency-stepped NMR; field-swept NMR. Molecular orbital calculations are used to correlate NMR spectra with geometry. Field-swept NMR spectroscopy has been most successful in establishing an upper bound for $C_q$ and differentiating between MAO-(gel) and MAO(solid). This technique finds an upper $C_q$ limit of about 22 MHz, depending on $\eta$, and therefore eliminates the possibility of 3-coordinate aluminum sites with their large $C_q$ values.

The upper and lower bounds for $^{27}$Al $C_q$ in MAO determined in this work add new interest in the use of MAS probes in resistive and hybrid magnet systems. Those fields of 33 and 45 T, when combined with 20−35 kHz spin rates, now seem to offer an excellent chance of success for resolving the long-standing structural questions associated with MAO.

**Acknowledgment.** The support of the National Science Foundation, Grant CHE-9977124, is gratefully acknowledged, as is funding for NMR and computer cluster equipment from the Louisiana Board of Regents. The Environmental Molecular Sciences Laboratory (a national scientific user facility sponsored by DOE Biological and Environmental Research) is located at Pacific Northwest National Laboratory and operated for the DOE by Battelle. The National High Magnetic Field Laboratory is sponsored by the National Science Foundation through Cooperative Agreement DMR-9527035 and by the State of Florida. We thank Rhonda Matthews and Brian Grant (Albemarle) and Charles Watkins (UAB) for generously supplying samples. We also thank Giuseppe Balacco for providing NMR processing software SwaN-MR (*J. Chem. Inf. Comput. Sci.* **1994**, *34*, 1235−1241).

JA011092A